Frequency Response Mismatch Correction in Multichannel Time Interleaved Analog Beamformers for Ultrasound Medical Imaging

Amir Zjajo
Circuits and Systems Group, Delft University of Technology, Delft, The Netherlands

Rene van Leuken
Circuits and Systems Group, Delft University of Technology, Delft, The Netherlands

ABSTRACT: Time interleaving is one of the most efficient techniques employed in the design of high-speed analog beamformers in ultrasound phased array transducers. However, its implementation introduces several mismatch errors between interleaved subunits, limiting the accuracy of the overall system. In this paper, a method for estimation and correction of frequency response mismatch based on an adaptive equalization is reported. The adaptive algorithm requires only that the input signal is band-limited to the Nyquist frequency for the complete system. The proposed method greatly reduce the computational complexity requirement of sampled signal reconstruction and offers simplified hardware implementation.

1 INTRODUCTION

The ultrasound imaging is frequently employed in medical diagnosis due to its real-time processing capability and less-detrimental effects to the human body in comparison with magnetic resonance imaging, computed tomography, and X-rays scanning. In the ultrasound phased array transducers, normally a beamforming (focusing) operation (Talman, 2003)-(Um, 2014) is performed to enhance the signal to noise ratio (SNR) of the ultrasound image. With the advances in analog delay lines and analog processing elements (e.g. analog-to-digital converters (ADC)), digital processing and digital beamforming was pushed completely into the front-end of a transducers. However, in modern transducers, a large number (e.g., 9216 for a 72×128 array) (Um, 2014) of transducer elements for active signal processing needs to be integrated in the ultrasound probe handle. As a consequence, due to the large number of required ADCs, digital beamforming becomes impractical and analog beamforming is necessary, at least at the front stage of the transducer.

The analog beamformer circuit consists of multiple, time-interleaved, analog sub-beamformers for sequential beamforming of multiple focal points on a scan line. Although time-interleaved principle provides efficient way to increase the conversion rate of sub-beamformers beyond the limit imposed by available technology on the maximum frequency of an overall beamformer, its implementation introduces several mismatch errors between interleaved units (Jenq, 1988), limiting the overall system accuracy. Offset, time and gain mismatches have been analyzed comprehensively (Petraglia, 1991), and in certain cases calibration/correction techniques have been proposed (Zou, 2011). The frequency response mismatch can be avoided through the use of a full-speed front-end sampler (Hsu, 2007). In this case, however, the sampler must be followed by a fast-settling buffer to drive the stages. Similarly, by increasing the bandwidth of interleaved sub analog beamformers, the impact of the frequency response mismatch at the signal frequency becomes lower, although at the cost of a severely reduced SNR.

Recently, iterative frequency response mismatch correction methods (Satarzadeh, 2009)-(Johansson, 2008) have been proposed based on adaptive filters either on each stage or at the system output by employing an inverse Fourier transform (Satarzadeh, 2009) or polynomial time varying filter structures (Johansson, 2008).

In this paper, we demonstrate digital frequency response mismatch correction in time-interleaved analog beamformer as an adaptive equalization process. The estimation method requires only that the input signal is band-limited to the Nyquist frequency for the complete system. The equivalent signal estimation structure can avoid aliasing without over sampling the input signal or operating at full sampling rate. The sparse structure of interleaved signals in the continuous frequency domain is used to replace the continuous reconstruction with a single finite dimensional problem. The implemented method significantly reduce the computational complexity requirement of sampled signal reconstruction and offers effective hardware implementation.

2 CORRECTION ALGORITHM

In the analog, time-interleaved beamformer, there are M identical sampling and sub-beamformers operating in parallel. Each subsystem samples and digitizes the input signal every MT seconds; i.e., the digitizing rate of each subsystem is $1/MT$ samples/s. Although all subsystems operate at the same clock frequency, the sampling clock of subsystem m+1 is T seconds behind that of the subsystem m for m =0,1,…,M-1. The timing alignment within the required accuracy is obtained by using a master clock to synchronize the different sampling instants. As illustrated in Figure 1, at the back end of these parallel sampling and sub-beamformers is a sequential M:1 multiplexer, which samples the outputs of beamformers stages at a rate of 1 sample/T s. The sub analog beamformer consists of a sample-and-hold circuit, which consists of sampling capacitors and switches and a clock controller. Time domain analog-beamformer output is shown in Figure 2. For M time-interleaved sub-beamformers, each working uniformly with a period of $T_s=MT$ and frequency response offset $\{h_m f_{in}/f_1=m_iT\}$, the clock generator provides the required M sample clocks for each sub-beamformer stage according to the sampling pattern such that $t_i(n)=(nM+m_i)=(n+m_i/M)T_s$ for $1\le i\le M$. Defining the i^{th} sampling sequence for $1\le i\le M$ as $x_{mi}[n]=x(t=nT=kMT+mT)$, the sequence of $x_{mi}[n]$ is obtained by up-sampling the output of the i-the sub-beamformer with a factor of M and shifting in time with m_i samples. The spectrum of the sampled time-domain signal is then represented as

$$
\begin{aligned}
Y_{mi}(e^{j2\pi fT}) &= \sum_{n=-\infty}^{+\infty} x_{mi}[n]e^{-j2\pi fT} = \frac{1}{MT}\sum_{k=0}^{M-1} A_k(f)X(f-\frac{k}{MT}) \\
&\forall f \in \mathcal{F}_0 = (0,\frac{1}{MT}), 1 \le i \le M \\
A_k(f) &= \sum_{n=0}^{M-1}\left(e^{-jnh_{m,i}f_{in}/f_1}\right)e^{-jkn(2\pi/M)}
\end{aligned}
\tag{1}
$$

where $Y_{mi}(e^{j2\pi fT})$ is the discrete-time Fourier transform (DTFT) *of* $x_{mi}[n]$ band-limited to $\mathcal{F}$, h_m for m=0,1,M-1 is frequency response mismatch encountered at the m-th unit, f_{in} is input frequency and f_1 the unity-gain frequency.

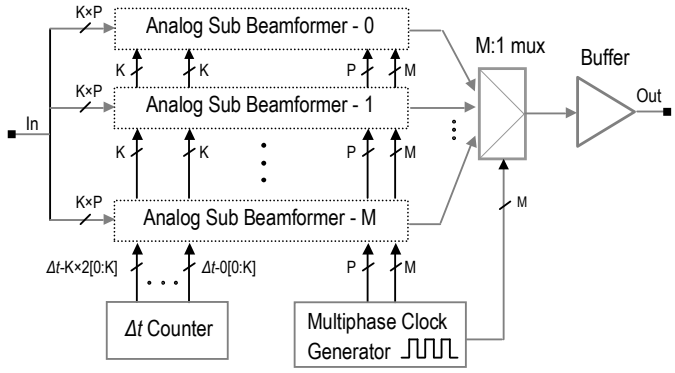

Figure 1: Analog beamformer architecture.

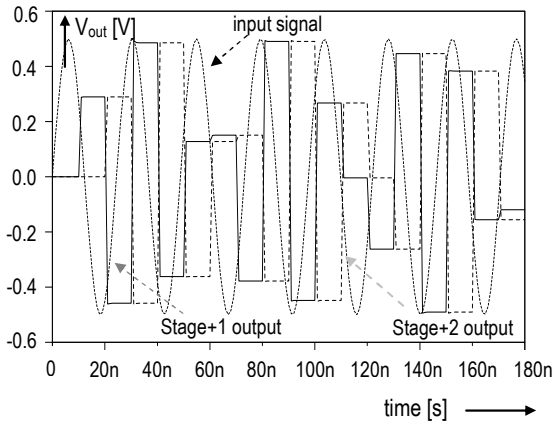

Figure 2: Time domain analog beamformer sample and hold output. For clarity M=3 is shown.

The goal of our reconstruction scheme is to perfectly recover $x(t)$ from the set of sequences of sampled signal $x_{mi}[n]$, $1 \le i \le M$. We express (1) in a matrix form as

$$\mathbf{y}(f) = \mathbf{A}(f)\mathbf{s}(f), \quad \forall f \in \mathcal{F}_0 \tag{2}$$

where $y(f)$ is a vector of length M whose i^{th} element is $Y_{mi}(e^{j2\pi fT})$,

$$\mathbf{y}(f)_{M\times 1} = [Y_1(e^{j2\pi fT}), Y_2(e^{j2\pi fT}), \ldots, Y_M(e^{j2\pi fT})]^T \tag{3}$$

$\mathbf{A}(f)$ is a the $M \times M$ discrete-time Fourier transform matrix containing $A_k(f)$ terms, and the vector $\mathbf{s}(f)$ contains M unknowns as (Mishali, 2009)

$$\mathbf{s}(f)_{M\times 1} = [X(f), X(f - 1/(MT)), \ldots, X(f - (M-1)/(MT))]^T, \forall f \in \mathcal{F}_0 \tag{4}$$

A straightforward approach to recover $x(t)$ is to find the sparsest vector $\mathbf{s}(f)$ over a dense grid of $\mathcal{F}_0$ and then approximate the solution over the entire continuous interval $\mathcal{F}_0$. However, this discretization strategy cannot guarantee perfect reconstruction. If we only need to reconstruct the distortion amplitudes at the nominal sampling instances $t=(kM+m)T_s$, $m=0,\ldots,M-1$; $k=0\ldots,-1,0,1,\ldots$ the reconstruction can be simplified. The spectrum given by (2) has M pairs of line spectra, each pairs centered at the fractional of the sampling frequency, such as $f_S/M,\ldots,(M-1)f_S/M$. Fundamental corresponds to k=0 while k=1,…,N-1 corresponds to the distortion. The signal amplitude is determined by $A(0)$ while the distortion amplitudes are determined by $A(n)$, $n=1,\ldots,M-1$. The spectral index set of the signal is than defined as the set $\mathbf{k}=[k_1, k_2, \ldots, k_q]$ and the reduced signal vector as (Bresler, 2008)

$$\mathbf{z}(f) = [X(f - k_1/M), X(f - k_2/M), \ldots, X(f - k_q/M)]^T \tag{5}$$

that contains only the q sampling instances indexed by the set k. The reduced measurement matrix $\mathbf{A}_k(f)$ is derived by choosing the columns of $\mathbf{A}_k(f)$ that are indexed by the spectral index k. Assuming $h_m f_{in}/f_1 \ll 1$ and using the first order Taylor expansion, the magnitude of the sidebands components (as illustrated in Figure 3 and Figure 4 (Zjajo, 2010)) can be expressed as

$$\left| A_k(f) = \sum_{n=0}^{M-1} (e^{-jh_m f_{in}/f_1}) e^{-jkn(2\pi/M)} \right| \approx \left| \frac{1}{M} \sum_{n=0}^{M-1} (1 - jh_m f_{in}/f_1) e^{-jkn(2\pi/M)} \right|$$

$$= \begin{cases} \dfrac{f_{in}}{Mf_1} \left| \displaystyle\sum_{n=0}^{M-1} h_m e^{-jkn(2\pi/M)} \right| & \text{for } k \neq 0, \pm M \\ \left| 1 - (jf_{in}/f_1)\left(\dfrac{1}{M} \displaystyle\sum_{n=0}^{M-1} h_m \right) \right| = 1 & \text{for } k = 0, \pm M \end{cases} \tag{6}$$

As a consequence, (2) reduces to

$$\mathbf{y}(f) = \mathbf{A}(f)\mathbf{z}(f), \quad \forall f \in \mathcal{F}_0 \tag{7}$$

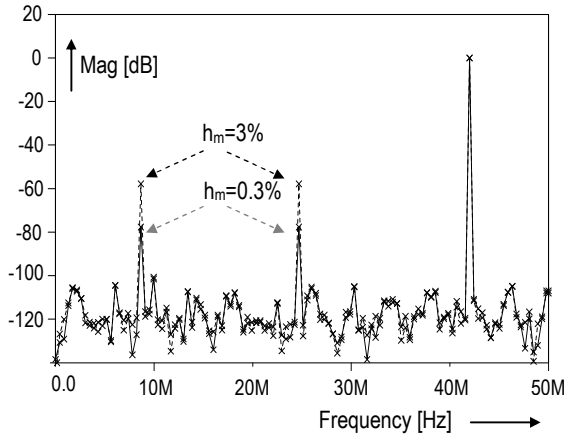

Figure 3: Simulated frequency response mismatch at h_m=0.3% and h_m =3% for f_{in}=41 MHz, f_s=100 MS/s and f_1=350 MHz.

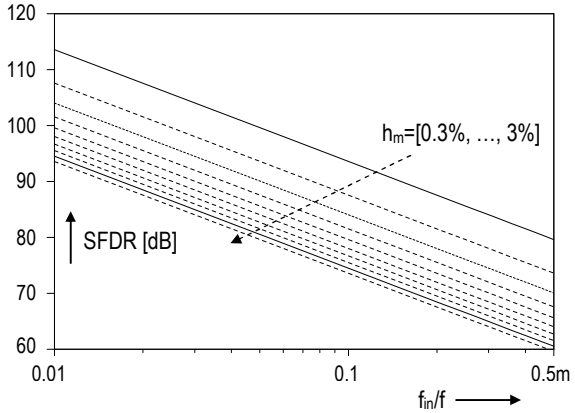

Figure 4: SFDR versus different frequency response ranging from h_m=0.3% to 3% for f_s=100 MS/s.

If $\boldsymbol{A}(f)$ has full column rank, the unique solution can be obtained using a left inverse, e.g. the pseudo-inverse of $\boldsymbol{A}(f)$ denoted by $\boldsymbol{A}^{\dagger}$

$$\mathbf{z}(f) = \mathbf{A}^{\dagger}(f)\mathbf{y}(f), \qquad \forall f \in \mathcal{F}_0 \tag{8}$$

A time domain solution for the recovery of $x(t)$ than involves filtering of the sequences $x_i[n]$, $i=1,\ldots M$ to generate $x_{hi}[n]$. The interpolation filter $h[n]$ with cut off frequency at $f_c=f_{max}/M$ filters the sequence $x_i[n]$ that is upsampled with M according to $kMT+mT$, i.e. $x_{hi}[n]=h[n]*x_i[n]$. To recover the desired continuous-time signal $x(t)$ with a standard D/A converter, the reconstruction is than obtained with

$$x(nT) = \sum_{i=1}^{q}\sum_{l=1}^{M}[\mathbf{A}^{\dagger}]_{il}\, x_{hl}[n] e^{j2\pi k_i n/M} \tag{9}$$

which is the Nyquist-rate sampled version of the desired continuous-time signal $x(t)$. Additionally, advantage of using (9) is that all filters have the same low pass response, offering efficient implementation. An estimation error can be than easily found by several methods from estimation theory (e.g. Gauss-Newton, Levenberg-Marquardt, or gradient search method) by comparing the estimated output $x(n)$ to a desired response.

3 EXPERIMENTAL RESULTS

The test results are shown in Figures 5-7 and Table I, where spurious-free dynamic range (SFDR) is employed as a performance matrix. The proposed approach achieves required reconstruction accuracy in less than one thousand samples for gradient search method (Figure 5).

TABLE I. EXAMPLE OF THE CALCULATED AND ESTIMATED SFDR VALUES

f_{in} [MHz]	43			57			71		
Δf_1 [MHz]	1	5	10	1	5	10	1	5	10
h_m [%]	0.29	1.42	2.86	0.29	1.42	2.86	0.29	1.42	2.86
Theor. [dB]	78.6	64.7	58.6	76.2	62.3	56.2	74.5	60.4	54.3
Est. [dB]	78.8	64.9	58.9	76.3	62.4	56.4	74.6	60.5	54.4

The iterative correction structure responses almost instantaneously with an improving estimate of mismatch parameters as *n* increases. To decrease the convergence time, initially a single set of coefficients is utilized and adapted after every decision, as in the conventional method, and then after initial convergence, the coefficients are further adapted separately. Validations have been performed for the entire analog beamformer usable signal bandwidth and most probable limitation mechanisms. Four examples are shown in Table I, where theoretical and estimated values are compared for 11, 43, 57 and 71 MHz input frequencies with unity gain frequency f_1 set at 350 MHz and deviations Δf_1 in the range of 1-10 MHz.

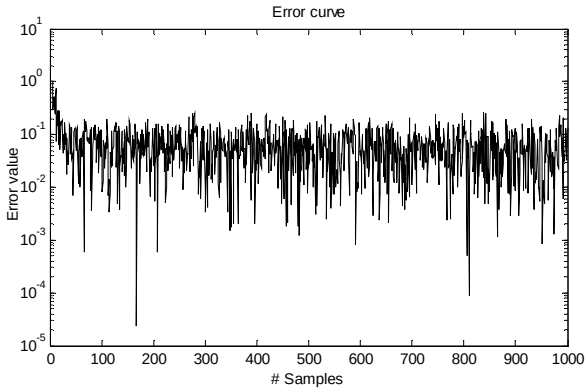

Figure 5: Mean-square error for one thousand samples.

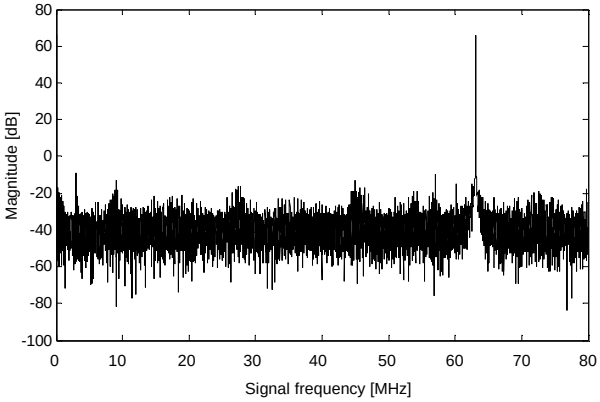

Figure 6: Spectrum of the time-interleaved beamformer at 160 MS/s.

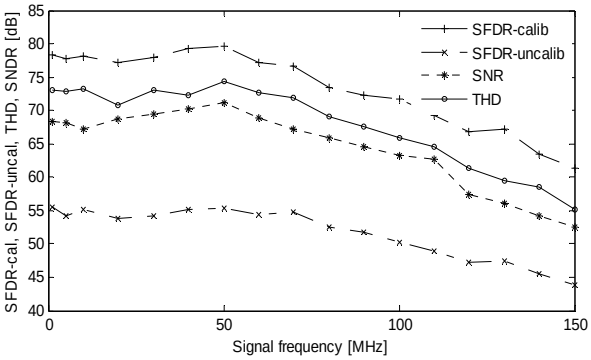

Figure 7: Measurement result of the time-interleaved beamformer at 160 MS/s.

The spectrum of the time-interleaved beamformer sampled at 160 MS/s is illustrated in Figure 6. The spurious harmonics at $f_s/N \pm f_{in}$ due to the frequency response mismatch are held to 72 dB below the fundamental signal. The SNR, SFDR and total harmonic distortion (THD) as a function of input frequency at a sample rate of 160 MS/s are shown in Figure 7. The uncalibrated beamformer SFDR is held below 56 dB, an average loss of 23 dB in comparison with calibrated beamformer. The calibration algorithm (0.5k gates) consumes 6 mW of power. All results are obtained with a 1.2 V supply at room temperature.

4 CONCLUSIONS

Combining time-interleaved analog beamformer with efficient, moderate speed converter result in a high speed ultrasound phased array transducer with low power consumption. Although parallelism of time-interleaved systems enables high-speed operation, mismatch between interleaved units, cause distortion in the processed signal. In this paper, effect of frequency response mismatch is investigated, and estimation method based on an adaptive equalization presented. Obtained results suggest that the proposed method accurately estimate (within 0.5%) and correct mismatch errors greatly enhancing analog beamformer performance (up to 23 dB).

REFERENCES

Bresler, Y. 2008. Spectrum-blind sampling and compressive sensing for continuous-index signals. *IEEE Information Theory and Applications Workshop*, pp. 547-554.

Gurun, G. *et al*., 2012. An Analog Integrated Circuit Beamformer for High-Frequency Medical Ultrasound Imaging. *IEEE Transactions on Biomedical Circuits and Systems*, vol. 6, pp. 454-467.

Hsu, C.C. *et al.*, 2007. An 11-b 800-MS/s time-interleaved ADC with digital background calibration. *IEEE International Solid-State Circuits Conference Digest of Technical Papers*, pp. 464-465.

Jenq, Y-C. 1988. Digital spectra of nonuniformly sampled signals: Fundamentals and high-speed waveform digitizers. *IEEE Transactions on Instrumentation and Measurement*, vol. 37, no. 2, pp. 245-251.

Johansson, H. & Lowenborg, P. 2008. A least-squares filter design technique for the compensation of frequency response mismatch errors in time-interleaved A/D converters. *IEEE Transactions on Circuits and Systems-II: Express Briefs*, vol. 55, no. 11, pp. 1154-1158.

Mishali, M. & Eldar, Y. 2009. Blind multiband signal reconstruction: compressed sensing for analog signals. *IEEE Transactions on Signal Processing*, vol. 57, pp. 993-1009.

Petraglia, A. & Mitra, S.K. 1991. Analysis of mismatch effects among A/D converters in a time-interleaved waveform digitizer. *IEEE Transactions on Instrumentation and Measurement*, vol. 40, no. 5, pp. 831-835.

Satarzadeh, P., Levy, B.C., Hurst, P.J. 2009. Adaptive semiblind calibration of bandwidth mismatch for two-channel time-interleaved ADCs. *IEEE Transactions on Circuits and Systems-I: Regular Papers*, vol. 56, no. 9, pp. 2075-2088.

Talman, J.R. *et al*., 2003. Integrated Circuit for High-Frequency Ultrasound Annular Array. *Proceedings of IEEE Custom Integrated Circuit Conference*, pp. 477-480.

Um, J.-Y. *et al*., 2012. A single-chip time-interleaved 32-channel analog beamformer for ultrasound medical imaging. *Proceedings of IEEE Asian Solid-State Circuits Conference*, pp. 193-196.

Um, J.-Y. *et al*., 2014. An analog-digital-hybrid single-chip RX beamformer with non-uniform sampling for 2D-CMUT ultrasound imaging to achieve wide dynamic range of delay and small chip area. *IEEE International Solid-State Circuits Conference Digest of Technical Papers*, pp. 426-427.

Zjajo, A., 2010. Design and Debugging of Multistep Analog to Digital Converters. *Eindhoven University of Technology*, PhD Thesis.

Zou, Y.X., Zhang, S.L., Lim, Y.C., Chen, X. 2011. Timing mismatch compensation in time-interleaved ADCs based on multichannel Lagrange polynomial interpolation. *IEEE Transactions on Instrumentation and Measurement*, vol. 60, no. 4, pp. 1123-1131.